Nonlinear solutions of plane Couette flow with and without a system rotation

Masato Nagata

Nonlinear solutions of plane Couette flow with and without a system rotation

Nagata Masato

Kyoto University
Department of Aeronautics and Astronautics, Graduate School of Engineering
Yoshida-honmachi, Sakyo-ku, Kyoto, 606-8501, Japan
nagata@kuaero.kyoto-u.ac.jp

Abstract :

We consider the bifurcation sequence of plane Couette flow with and without a system rotation. First, we mention briefly how the finite amplitude solutions in plane Couette flow, which is linearly stable at any Reynolds number and therefore no bifurcation from the basic state exists, are obtained as the solutions at zero-rotation rate of the tertiary flow in the rotating case. Secondly, the stability analysis of the tertiary flow is described, where the stable solutions undergo Hopf bifurcations as the rotation rate is varied. Then, we report on our recent theoretical development of the problem, namely, detecting periodic solutions arising from the Hopf bifurcations and their homoclinic connection in the rotating case. We provide experimental observations to support our theoretical findings. Finally, the existence of periodic solutions on the axis of the zero-rotation rate, i.e. plane Couette flow, will be demonstrated by continuing the periodic solution branch of the rotating case.

Key-words :

transition ; instability ; plane Couette flow

1 Introduction

Plane Couette flow without a system rotation is known to be linearly stable at any finite values of the Reynolds number, Re, thus indicating no direct bifurcation from the basic state with a linear velocity profile. Nagata (1990) analysed the nonlinear stability of the flow by adding a system rotation, Ω, in the spanwise direction and successfully continued a tertiary flow branch of the rotational system to the non-rotating case in the (Ω, Re)-space, discovering a 3D nonlinear steady solution of plane Couette flow for the first time (see Figure 1). Later, Nagata (1998) showed that the tertiary flow branch of the rotating system is stable for relatively small Reynolds numbers, and that oscillatory instabilities begin to emerge in the middle of the stable branch of the tertiary flow as the Reynolds number is increased. As the Reynolds number is further increased the interval of the oscillatory instability bounded by a Hopf bifurcation point at its both ends spreads in the direction of both increasing and decreasing rotation number Ω.

We obtain periodic solutions bifurcating from the Hopf bifurcation points by using a Newton-Raphson iterative method to find a fixed point on the Poincaré cross-section. When the Reynolds number is small the Hopf bifurcation points are connected by a periodic solution branch. For a larger Reynolds number, however, the periodic solution collides with the secondary flow (two-dimensional streamwise vortex flow), forming a homoclinic connection as the rotation rate is varied.

2 Mathematical formulation

We consider a viscous incompressible fluid motion between two parallel plates separated by the distance L. One of the plates moves along in its own plane with a constant speed $\frac{1}{2}U_0$, whereas

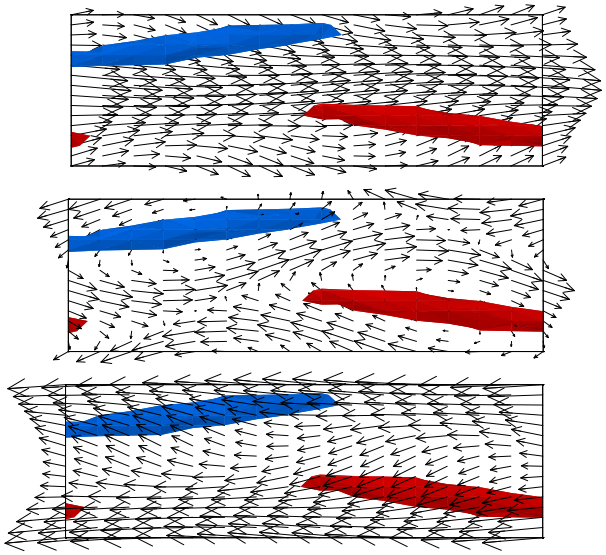

Figure 1: The steady three-dimensional finite-amplitude solution of plane Couette flow at $Re = 600$ and $\Omega = 0$. The velocity field projected on the planes, $z = 0.25$ (top), $z = 0$ (middle) and $z = -0.25$ (bottom), is indicated by arrows. The regions of the strong sreamwise vorticity are indicated by dark(positive) and light(negative) grey areas.

the other moves in the opposite direction with the same speed. A constant spanwise rotation Ω_0 is imposed on the system. By using L as the length scale, L^2/ν as the time scale where ν is the kinematic viscosity, and ν/L as the velocity scale, we can express the laminar solution by

$$U_B(z) = Re\, z, \tag{1}$$

where z is the coordinate in the direction normal to the plates and Re is the Reynolds number defined by $Re = U_0 L/\nu$. The non-dimensional basic equations for the velocity $\boldsymbol{u}$ and the pressure p deviated from the laminar state are given by

$$\nabla \cdot \boldsymbol{u} = \boldsymbol{0}, \tag{2}$$

$$\frac{\partial \boldsymbol{u}}{\partial t} + (U_B \boldsymbol{i} \cdot \nabla \boldsymbol{u}) + \boldsymbol{u} \cdot \nabla (U_B \boldsymbol{i}) + \boldsymbol{u} \cdot \nabla \boldsymbol{u} = -\nabla p + \nabla^2 \boldsymbol{u} - \Omega \boldsymbol{j} \times \boldsymbol{u}, \tag{3}$$

where $\boldsymbol{i}$ and $\boldsymbol{j}$ are the unit vectors in the streamwise and spanwise directions, respectively, and Ω is the rotation number defined by

$$\Omega = 2\Omega_0 L^2/\nu. \tag{4}$$

The no-slip boundary conditions on the plates are imposed:

$$\boldsymbol{u} = \boldsymbol{0} \quad \text{at} \quad z = \pm 1/2. \tag{5}$$

Thus, the nonlinear development of $\boldsymbol{u}$ is governed by two non-dimensional parameters, the Reynolds number Re and the rotation number Ω (see Nagata (1990,1998)).

For convenience we separate the velocity deviation $\boldsymbol{u}$ into the average part $\check{U}(z)$ and the spatially-periodic residual $\check{\boldsymbol{u}}$. As the nonlinear measure of the finite-amplitude solution we choose the momentum transport τ on the boundaries defined by

$$\tau = \frac{\frac{d}{dz}[U_0(\pm\frac{1}{2}) + \check{U}(\pm\frac{1}{2})]}{\frac{d}{dz}U_0(\pm\frac{1}{2})}. \tag{6}$$

3 Numerical Methods

In the present analysis we use three different numerical schemes as described below.

1. Newton-Raphson method for steady motions:

   The disturbance of a steady motion is expressed by the Fourier expansions in the streamwise and spanwise directions and the Chebyshev-polynomial expansions in the direction normal to the plates. Substitution of the expansions to the basic equations reduces to a set of nonlinear algebraic equations for the expansion coefficients with the aid of the Chebyshev collocation method. We employ the Newton-Raphson iterative method to solve the equations. The stability of steady motions is evaluated by applying Floquet theory.

2. DNS:

   The time development of the disturbance is followed by a direct numerical simulation (DNS), where the time integration is performed on the full Navier-Stokes equation by using a pseudo-spectral method. The numerical scheme for the simulation is essentially the same as the one used by Kim, Moin & Moser (1987).

3. Newton-Raphson method for periodic motions:

   For time-periodic solutions we employ Newton-Raphson computation of a fixed point in a Poincaré map. The one-period time integration of the Navier-Stokes equation for the Poincaré map, is computed by the DNS. The Jacobian matrix is evaluated by a finite-difference approximation. We use a stable periodic state, which is accessible to the DNS, as an initial guess for the Newton–Raphson iteration and extend it to an unstable region in the parameter space.

4 Analysis

4.1 3D steady solutions

Figure 2(a) shows the variation of the momentum transport τ against Ω for various types of motions when $Re = 400$. The solid curve indicates the two-dimensional streamwise vortex flow branch with the streamwise wavenumber $\alpha = 0$ and the spanwise wavenumber $\beta = 3.117$, whereas the dotted curve indicates the steady three-dimensional flow branch with $\alpha = 1.0$ and $\beta = 3.117$. They are obtained by the Newton-Raphson method. Steady flows obtained by the DNS are indicated by open circles. We can see that as Re is increased from zero the stable streamwise vortex flow, which bifurcates from the laminar flow at $\Omega = \Omega_{\mathbf{C}}(= 4.3)$, becomes unstable at $\Omega = \Omega_1(= 6.5)$ and the stability is taken over by the steady three-dimensional flow. On the other hand, when Ω is decreased from a large value, the stable streamwise vortex flow becomes unstable at $\Omega = \Omega_2(= 47)$ and the stability is again taken over by the steady three-dimensional flow.

As Re is increased the steady three-dimensional flow branch gradually deforms in such a way that it is pulled towards a smaller Ω by keeping its feet at $\Omega = \Omega_1$ and $\Omega = \Omega_2$ still on the streamwise vortex flow branch until the middle section of the branch passes through the line of $\Omega = 0$, creating two intersections on the τ-axis (see Nagata (1990)). In fact, the steady three-dimensional solution at $Re = 600$ shown in Figure 1 corresponds to the solution at the upper intersection.

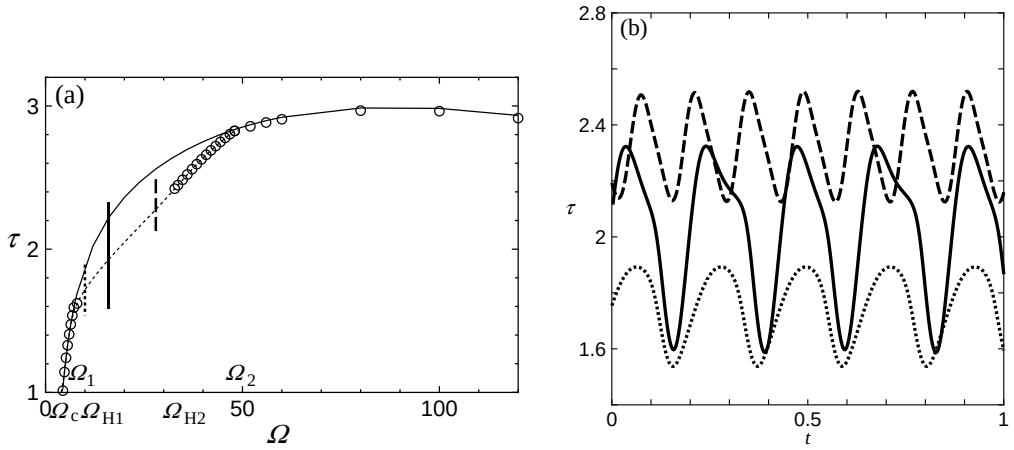

Figure 2: (a) The momentum transport τ against the rotation number Ω for various types of motions. $Re = 400$. (b) The time development of τ for three periodic motions at Ω =10 (dotted curve), 16 (thick curve) and 28 (dashed curve).

4.2 Stability of the 3D steady solutions

Recently, Nagata (1998) investigated the stability of the tertiary flow in rotating plane Couette flow. He found that the tertiary flow is stable for a relatively small Re. As Re is increased, however, the stability of the steady three-dimensional flow is destroyed by oscillatory instabilities gradually from the middle of the solution branch between Ω_1 and Ω_2, and the unstable region spreads with the Hopf bifurcation points, $\Omega = \Omega_{\mathrm{H1}}$ and $\Omega = \Omega_{\mathrm{H2}}$, at its ends. The instability region for $Re = 400$ expands between $\Omega_{\mathrm{H1}} = 8.4$ and $\Omega_{\mathrm{H2}} = 32$ as shown in Figure 2(a).

4.3 Time-dependent solutions

4.3.1 Periodic solutions

We follow the time-dependent fluid motion resulting from Hopf bifurcations at $\Omega = \Omega_{\mathrm{H1}}$ and $\Omega = \Omega_{\mathrm{H2}}$ by DNS. It is found that for $Re = 400$ the time-dependent motion is characterised by periodic motions (P1) when Ω is near both Ω_{H1} and Ω_{H2}: the dotted and dashed vertical lines in Figure 2(a) represent the periodic motions at $\Omega = 10$ and $\Omega = 28$, respectively. The time development of these periodic motions are indicated by the dotted and dashed curves, respectively, in Figure 2(b). When Ω is away from Ω_{H1} or Ω_{H2}, there exists a new periodic motion (P2) with twice the period of P1 as shown by the solid vertical line at $\Omega = 16$ in Figure 2(a) and by the solid curve in Figure 2(b).

4.3.2 Homoclinic connection

The period of the periodic solution, P1, which has bifurcated at Ω_{H1} becomes infinite as Ω approaches Ω_{HOM1} as can be seen in Figure 3. Similarly, the period of the periodic solution, P1, which has bifurcated at Ω_{H2} becomes infinite as Ω approaches Ω_{HOM2}. The periodic solutions, P2 with twice the period, exist between Ω_{HOM1} and Ω_{HOM2} and their period also becomes infinite as Ω approaches either Ω_{HOM1} or Ω_{HOM2}. The trajectories of the periodic solutions, P1 and P2, are projected on a two-dimensional plane with the two imaginary parts of the three-dimensional component, ω_z, of the vorticity, $\mathrm{Im}(\omega_{z1,0,0})$ and $\mathrm{Im}(\omega_{z1,0,2})$, as its coordinates in Figure 4. The trajectory of the periodic solution, P1, is plotted at Ω slightly smaller than Ω_{HOM1} and the tra-

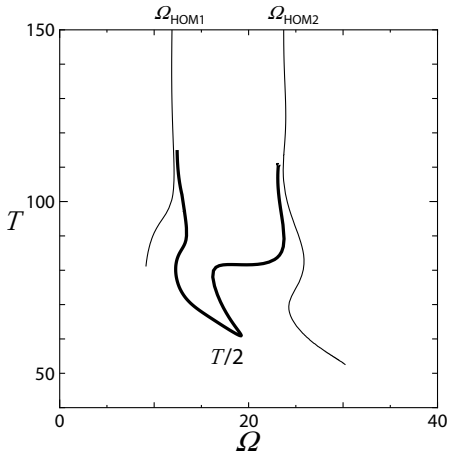

Figure 3: The period, T, of the periodic motions at $Re = 400$. The thin curves represent the periodic solution (P1) and the thick curve represents the periodic solution (P2) with twice the period.

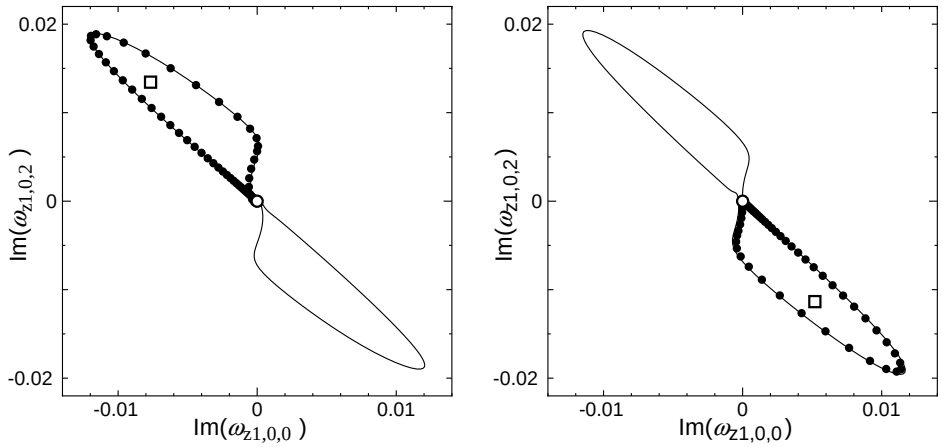

Figure 4: The trajectories of the periodic solutions, P1 (dots) and P2 (curve). The circle indicates the two-dimensional streamwise flow whereas the square represents the three-dimensional steady solution. (Left):$\Omega \approx \Omega_{\mathrm{H1}}$. (Right):$\Omega \approx \Omega_{\mathrm{H2}}$

jectory of the periodic solution, P2, is drawn at Ω slightly lager than Ω_{HOM1} in Figure 4:(Left). Similarly, The trajectories of P1 and P2 are plotted at Ω slightly larger and smaller, respectively, than Ω_{HOM2} in Figure 4:(Right). It is seen that the periodic solutions collide with the streamwise vortex flow when Ω approaches either Ω_{HOM1} or Ω_{HOM2}, forming a homoclinic connection with the unstable two-dimensional streamwise vortex flow.

4.3.3 3D periodic solutions in plane Couette flow

Starting from the periodic solution detected at $(\Omega, Re) = (10, 400)$ (see Figure 2) we trace the periodic motion, P1, in the (Ω, Re)-space by keeping the period T constant (i.e. $T = 90.8$) as indicated by the curve in Figure 5:(Left). As we can see the curve extends to a smaller Ω and crosses the line of $\Omega = 0$ at $Re = 774$. The solution at the intersection with the line of $\Omega = 0$ corresponds to the periodic motion for non-rotating plane Couette system. The detected periodic motion is followed along $\Omega = 0$ in the direction of smaller Re as shown in Figure 5:(Right). It is found that the periodic solution of plane Couette flow bifurcates from the steady

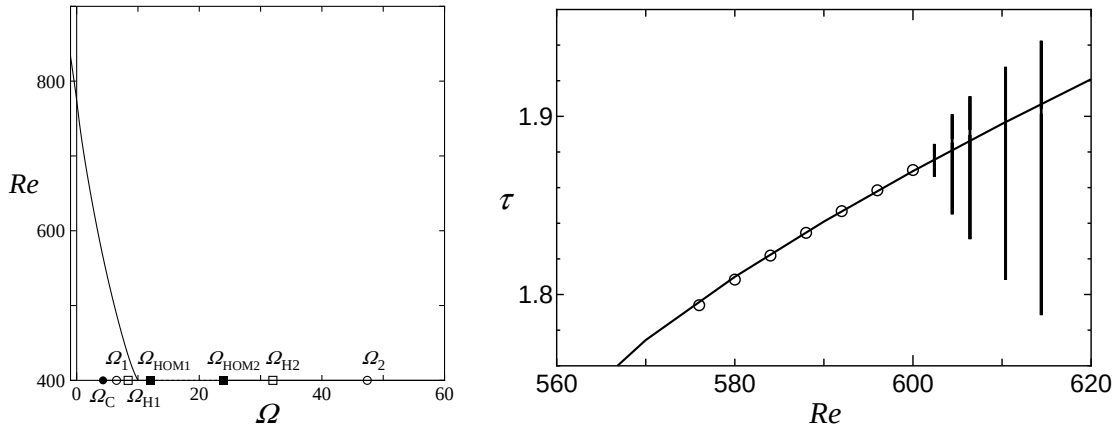

Figure 5: (Left): The trace of the periodic solution with the period $T = 90.8$ in the (Ω, Re)-space. (Right): The bifurcation of the periodic solution (vertical lines by Newton-Raphson method on the Poincaré section) from the steady three-dimensional flow (curve by Newton-Raphson method and circles by DNS) in plane Couette flow.

three-dimensional solution at $Re = 610$.

5 Conclusion

We have shown that the periodic motions, which bifurcate from the tertiary flow branch in the rotating plane Couette system, undergo a homoclinic connection with the streamwise vortex flow. The experimental observations by Hiwatashi *et al*.(2006) support our theoretical findings described above.

We have traced the periodic motions in the (Ω, Re)-space and found that they exist even when the system rotation is absent. Preliminary investigation has indicated that the periodic motions of plane Couette system obtained in the present paper do not have connection with those found by Clever & Busse (1997) or Kawahara & Kida (2001).

References

Clever, R. M., Busse, F. H. 1997 Tertiary and Quaternary solutions for plane Couette flow. *J. Fluid Mech.* **344** 137-153

Hiwatashi, K., Alfredsson, P. H., Tillmark, N., Nagata, M. 2006 Experimental observation in rotating plane Couette flow. *Phys. Fluids*, Submitted.

Kawahara, G., Kida, S. 2001 Periodic motion embedded in plane Couette turbulence: regeneration cycle and burst. *J. Fluid Mech.* **449** 291-300

Kim, J., Moin, P., Moser, R. 1987 Turbulence statistics in fully developed channel flow at low Reynolds number. *J. Fluid Mech.* **177** 133-166

Nagata, M. 1990 Three-dimensional finite amplitude solutions in plane Couette flow: bifurcation from infinity. *J. Fluid Mech.* **217** 519-527

Nagata, M. 1998 Tertiary solutions and their stability in rotating plane Couette flow. *J. Fluid Mech.* **358** 357-378